Macromolecules

ARTICLE

pubs.acs.org/Macromolecules

Enzymatic Surface Hydrolysis of PET: Effect of Structural Diversity on Kinetic Properties of Cutinases from *Thermobifida*

Enrique Herrero Acero,[†] Doris Ribitsch,[†,*] Georg Steinkellner,[†] Karl Gruber,[†,‡] Katrin Greimel,[†] Inge Eiteljoerg,[†] Eva Trotscha,[†] Ren Wei,[§] Wolfgang Zimmermann,[§] Manfred Zinn,[⊥] Artur Cavaco-Paulo,[∥] Giuliano Freddi,[○] Helmut Schwab,[†,▽] and Georg Guebitz[†,#]

[†]Austrian Centre of Industrial Biotechnology ACIB, Graz, Austria

[‡]Institute of Molecular Biosciences, University of Graz, Graz, Austria

[§]Department of Microbiology and Bioprocess Technology, Institute of Biochemistry, University of Leipzig, Leipzig, Germany

[⊥]Laboratory for Biomaterials, Swiss Federal Laboratories for Materials Science and Technology (Empa), St. Gallen, Switzerland

[∥]Textile Engineering Department, University of Minho, Guimarães, Portugal

[○]Stazione Sperimentale per la Seta, Milano, Italy

[▽]Institute of Molecular Biotechnology, Graz University of Technology, Graz, Austria

[#]Institut for Environmental Biotechnology, Graz University of Technology, Graz, Austria

ABSTRACT: In this study cutinases from *Thermobifida cellulosilytica* DSM44535 (Thc_Cut1 and Thc_Cut2) and *Thermobifida fusca* DSM44342 (Thf42_Cut1) hydrolyzing poly(ethylene terephthalate) (PET) were successfully cloned and expressed in *E.coli* BL21-Gold(DE3). Their ability to hydrolyze PET was compared with other enzymes hydrolyzing natural polyesters, including the PHA depolymerase (ePhaZmcl) from *Pseudomonas fluorescens* and two cutinases from *T. fusca* KW3. The three isolated *Thermobifida* cutinases are very similar (only a maximum of 18 amino acid differences) but yet had different kinetic parameters on soluble substrates. Their k_{cat} and K_m values on pNP−acetate were in the ranges 2.4−211.9 s^{-1} and 127−200 μM while on pNP−butyrate they showed k_{cat} and K_m values between 5.3 and 195.1 s^{-1} and between 1483 and 2133 μM. Thc_Cut1 released highest amounts of MHET and terephthalic acid from PET and bis(benzoyloxyethyl) terephthalate (3PET) with the highest concomitant increase in PET hydrophilicity as indicated by water contact angle (WCA) decreases. FTIR-ATR analysis revealed an increase in the crystallinity index A_{1340}/A_{1410} upon enzyme treatment and an increase of the amount of carboxylic and hydroxylic was measured using derivatization with 2-(bromomethyl)naphthalene. Modeling the covalently bound tetrahedral intermediate consisting of cutinase and 3PET indicated that the active site His-209 is in the proximity of the O of the substrate thus allowing hydrolysis. On the other hand, the models indicated that regions of Thc_Cut1 and Thc_Cut2 which differed in electrostatic and in hydrophobic surface properties were able to reach/interact with PET which may explain their different hydrolysis efficiencies.

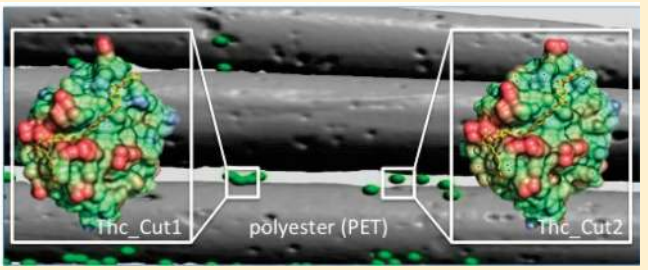

1. INTRODUCTION

Among the manmade polymers, PET is one of the most widely used polymer worldwide and its use ranges from containers, medical applications,[1] or fibers for textiles which account for more than 50% of all fibers in 2000.[2] On the other hand a main drawback results from the highly hydrophobicity of PET which makes the polymer difficult to be functionalized. Therefore, industrial applications require activation of the surface prior to final treatment. Currently, plasma or wet chemistry methods persuade to insert hydrophilic moieties like carboxylic or hydroxyl groups onto the surface. However, plasma treatments are very energy consuming and it is a well-known that after the treatment the created surface polar groups are instable leading to a hydrophobicity regain.[3,4] Chemical methods normally involve environmentally harmful substances[5,6] and in some cases they lead to a decrease of polymer weight (up to 15%) and of strength properties.[7] PET−hydrolases hydrolyze the ester bond of PET thereby releasing terephtahlic acid (TA), ethylene glycol (EG) and oligomers like MHET and BHET.[7] In addition, PET−hydrolases hydrolyze internal ester bonds endowise increasing the hydrophilicity of the polymer.[7−9]

Enzymatic modification of synthetic polymers has attracted the attention of several research groups in the recent years.[10−13] The substitution of harsh chemicals by enzymes would avoid damaging of the fibres and could be performed environmentally friendly and under energy saving process conditions.[14] Cutinases have been suggested both for PET recycling[15] and for antipilling

Received: April 28, 2011
Revised: May 11, 2011
Published: May 20, 2011

treatment in detergents.[16,17] As detergent components cutinases additionally reduce redeposition of stains on PET fibers when used in multiple washing cycles.[18]

Enzymes able to hydrolyze PET include esterases,[19] lipases,[20,21] cutinases from *Humicola insolens*,[22] *Fusarium solani pisi*,[23] *Fusarium oxysporum*,[24] *Penicillium citrinum*,[25] *Pseudomonas mendocina*,[22] and from different *Thermobifida* species.[9,26,27] Interestingly, even among one enzyme class (i.e., cutinases), individual representatives showed considerably different activities on PET.[22] Thus, in order to engineer or screen for more efficient PET-hydrolases more knowledge about structure function relationships of these enzymes will be essential. Here we compared closely related cutinases from *T. cellulosilytica* DSM44535 (Thc_Cut1 and Thc_Cut2), and *T. fusca* DSM44342 (Thf42_Cut1) regarding PET-hydrolysis. Their surprisingly distinct catalytic properties both on PET and small molecules were correlated to structural differences. In addition, these cutinases were compared with other enzymes previously described for PET-hydrolysis including the PHA depolymerase from *P. fluorescens*[28,29] and two cutinases from *T. fusca* (ThfKW3_Cut1 and ThfKW3_Cut2, GenBank FR727680 and FR727681) in their ability of hydrolyzing PET films.

2. MATERIALS AND METHODS

2.1. Chemicals and Enzymes. Methanol, acetonitrile were purchased from Roth (Carl Roth GmbH, Karlsruhe, Germany). All other chemicals were of analytical grade from SIGMA (Germany) except the model substrate bis(benzoyloxyethyl) terephthalate (3PET) which was synthetized in two steps as previously described.[30] The PHA-depolymerase from *P. fluorescens* ePhaZmcl and ThfKW3_Cut1 and ThfKW3_Cut2 from *T. fusca* were produced and purified as previously described.[28,31] PET films were kindly provided by Dr. Vincent Nierstrasz from Ghent University. PET had a crystallinity degree of 37% measured by DSC.[21]

2.2. Bacterial Strains, Plasmids, and Culture Conditions. *T. cellulosilytica* DSM44535 and *T. fusca* DSM44342 were obtained from the German Resource Centre for Biological Material (DSMZ, Germany). The strains were maintained on LB/agar plates and cultivated in 500 mL shaking flasks (200 mL LB medium) at 37 °C and 160 rpm for 24 h. Cells were harvested by centrifugation at 3,200*g* and 4 °C for 20 min. Vector pET26b(+) (Novagen, Germany) was used for expression of enzymes in *Escherichia coli* BL21-Gold (DE3) (Stratagene, Germany).

2.3. General Recombinant DNA Techniques. All DNA manipulations described in this work were performed by standard methods.[32] The PCR was performed in a Gene Amp PCR 2200 thermocycler (Applied Biosystems, USA). Digestion of DNA with restriction endonucleases (New England Biolabs, USA), dephosphorylation with alkaline phosphatase (Roche, Germany) and ligation with T4 DNA-ligase (Fermentas, Germany) were performed in accordance to the manufacturer's instructions. Plasmid Mini Kit from Qiagen (Germany) was used to prepare plasmid DNA. Plasmids and DNA fragments were purified by Qiagen DNA purification kits (Qiagen, Germany).

2.4. Construction of Cutinase Genes. The genes Thc_cut1, Thc_cut2, and Thf42_cut1 coding for cutinases were amplified from the respective genomic DNA of *T. cellulosilytica* DSM44535 and *T. fusca* DSM44342 by standard polymerase chain reaction (PCR). On the basis of the known sequence of genes coding for cutinases from *T. fusca* YX (Genbank accession numbers YP_288944 and YP_288943,[33]) two primers were designed, 5′-CCCCCGCTCATATGGCCAACCCCTACGAGCG-3′ (forward primer) and 5′-GTGTTCTAAGCTTCAGTGGTGGT-GGTGGTGGTGCTCGAGTGCCAGGC ACTGAGAGTAGT- (reverse primer), allowing amplification of the respective gene without signal peptide and introduction of the 6xHis-Tag at the C-terminus of the cutinases. The designed primers included restriction sites *Nde*I and *Hind*III for cloning the gene into the vector pET26b(+). The PCR was done in a volume of 50 μL with genomic DNA as template, 0.4 μM of each primer, 0.2 mM dNTP's, 5 units Phusion DNA polymerase (Finnzymes) and 1× reaction buffer provided by the supplier. A total of 35 cycles were done, each cycle with sequential exposure of the reaction mixture to 98 °C (30 s, denaturation), 63 °C (30 s, annealing), and 72 °C (30 s, extension). The amplified PCR-products thus obtained were purified, digested with *Nde*I and *Hind*III, ligated to pET26b(+) and transformed in *E. coli* BL21-Gold(DE3). The sequences of the genes were determined by DNA sequencing using the primers 5′-GAGCGGATAACAATT CCCCTCTA-GAA-3′ and 5′-CAGCTTCCTTTCGGGCTTTGT-3′.

2.5. DNA Sequencing, Alignments, and Deposition of Sequence Data. DNA was sequenced as custom service (Agowa, Germany). Analysis and handling of DNA sequences was performed with Vector NTi Suite 10 (Invitrogen, USA). Sequences of proteins were aligned using the Clustal W program (Swiss EMBnet node server). The nucleotide sequences of the isolated genes has been deposited in the GenBank database under accession numbers HQ147785 (Thc_cut1), HQ147786 (Thc_cut2), and HQ147787 (Thf42_cut1).

2.6. Expression and Purification of Cutinases. Freshly transformed *E. coli* BL21-Gold(DE3) cells were used to inoculate 20 mL of LB-medium supplemented with 40 μg/mL kanamycin. The culture was grown overnight on a rotary shaker at 30 °C and 160 rpm. Then, 1 mL of the overnight culture was transferred to a 500 mL shaking flask containing 200 mL of the same liquid medium and incubated at 30 °C until an optical density (600 nm) between 0.6 and 0.8 was reached. The culture was cooled down to 20 °C and induced with IPTG at a final concentration of 0.05 mM. The induced culture was incubated overnight at 20 °C and 160 rpm. The cells were harvested by centrifugation (3200*g*, 4 °C, 20 min).

Cell pellet from 100 mL of cell culture was resuspended in 10 mL buffer (50 mM NaH_2PO_4, 300 mM NaCl, 10 mM imidazol, pH 8.0) and sonicated with three-times 30-s pulses under ice cooling using a cell disruptor from BRANSON Ultrasonics. The enzymes were purified by affinity chromatography. For this purpose the 6xHis peptide was C-terminally fused over an Ala-Leu-Glu linker sequence to the cutinases. Purification was done according to the manufacturer's protocol. For characterization of cutinases the HisTag elution buffer was exchanged with 100 mM Tris HCl pH 7.0 by the use of PD-10 desalting columns (Amersham Biosciences).

2.7. Protein Quantification and SDS−PAGE Analysis. Protein concentrations were determined by the Uptima BC Assay protein quantification kit from Interchim (France) and bovine albumin as protein standard. SDS−PAGE was performed corresponding to Laemmli,[34] proteins were stained with Coomassie Brillant Blue R-250.

2.8. Activity Assay. Esterase activity was measured at 25 °C using p-nitrophenyl acetate (PNPA) and *p*-nitrophenyl butyrate (PNPB) as a substrate. The final assay mixture consisted of a volume of 200 μL of the substrate solution diluted in 50 mM phosphate buffer at pH = 7 and 20 μL of enzyme solution.

The increase of the absorbance at 405 nm was measured using a Tecan INFINITE M200 plate reader. A blank was measured using

20 μL buffer instead of sample. The increase of the absorbance indicated an increase of *p*-nitrophenol (ε_{405nm} = 11.86 $mmol^{-1}$ cm^{-1}) due to hydrolysis of the PNPA or PNPB. The activity was calculated in units, where 1 unit had been defined as being the amount of enzyme required to hydrolyze 1 μmol of substrate per minute under the given assay condition.

The Michaelis−Menten parameters K_m, and V_{max} were determinded by using the corresponding substrate at 25 °C and pH = 7. Calculations were made by using the software "Origin", version 4.10.

2.9. 3PET and PET Hydrolysis. The hydrolysis of the PET model substrate 3PET was performed as previously described.[30] In the case of 3PET before incubation the powder was filtered in order to homogenize the size of the polymer particles. In each sample 400 μL of the corresponding enzyme solution (dosage was 6.75 μM diluted 1:1 with buffer K_2HPO_4/KH_2PO_4) was incubated with 10 mg 3PET for 72 h. On the basis of previous studies on Thc_Cut1 and Thc_Cut2[33,35] 50 °C was chosen because the enzyme retains good stabilty and activity. In addition, a higher temperature would increase the mobility of the polymer chains which has been proven to increase the enzymatic polymer hydrolysis.[9] A pH value of 7 has been found to be suitable in many studies[7,9,20] with Thc_Cut1 and Thc_Cut2.

Thereafter proteins were precipitated using 1:1 (v/v) methanol abs. on ice. Samples were centrifuged (Hettich MIKRO 200 R, Tuttlingen, Germany) at 16,000*g* at 0 °C for 15 min .The supernatant for measurement was brought to an HPLC vial and acidified by adding 1 μL of HCl concentrated. The HPLC used was a DIONEX P-580 PUMP (Dionex Cooperation, Sunnyvale, USA), with an ASI-100 automated sample injector and a PDA-100 photodiode array detector. For analysis of TA, benzoic acid (BA), 2-hydroxyethyl benzoate (HEB), mono-(2-hydroxyethyl) terephthalate (MHET) and bis(2-hydroxyethyl) terephthalate (BHET) a reversed phase column RP-C18 (Discovery HS-C18, 5 μm, 150 × 4.6 mm with precolumn, Supelco, Bellefonte, USA) was used. Analysis was carried out with 20% acetonitrile, 20% 10 mM sulfuric acid and 60% (v/v) water as eluent. The flow rate was set to 1 mL min^{-1} and the column was maintained at a temperature of 25 °C. The injection volume was 10 μL. Detection of the analytes was performed with a photodiode array detector at the wavelength of 241 nm.

Prior to the enzyme treatment PET films were cut into pieces as specified below and washed in three consecutive steps. In a first step, each PET piece was washed with a solution of Triton-X100, in a next step 100 mM Na_2CO_3 and finally deionized water was used. For water contact angle (WCA) determinations PET films were cut in 10 mm diameter disks and incubated in 15 mL glass beakers with 4 mL of enzyme solution. For crystallinity determinations and fluorescence spectroscopy the polymer treatment involved incubation off a piece of PET films (100 × 10 mm) in a 15 mL falcon tube with 13 mL of enzyme solution in order to keep the ratio surface/enzyme constant. In both cases, the conditions were 6.75 μM enzyme concentration, at 130 rpm and 50 °C for 120 h. Hydrolysis products were measured by HPLC with the same procedure as for 3PET in samples incubated for water contact angle measurements.

2.10. Water Contact Angle. Contact angles of the PET film after exposure to enzymes were measured as previously reported[20] after two aditional washing steps. In a first step a 30 min wash with Sodium Dodecyl Sulfate (SDS) at 35 °C was done followed by a 30 min wash with destilled water at 35 °C. Polymer films were analyzed with the Drop Shape Analysis System DSA 100 (Kruss GmbH, Hamburg, Germany) using deionized water as test liquid with a drop size of 3 μL. Contact angles were measured after 3 s and data are obtained from the averages of the measurements taken from 15 different points of the sample surface

2.11. Fluorescence Spectroscopy. PET films of 50 × 10 mm size were alkylated in 20 mL of *N*,*N*-dimethylformamide (DMF) containing 2-(bromomethyl)naphthalene (0.05 M) and potassium fluoride (0.02 M). Samples were incubated for 3 h at room temperature under shaking conditions at 100 rpm. Thereafter PET films were washed with DMF in order to remove unreacted reagents and then rinsed with distilled water. Samples were dried at room temperature and the fluorescence emission was measured using a multiplate reader (Varioskan, Thermo) with excitation and emission wavelengths of 350 and 440 nm, respectively.

2.12. FTIR. Fourier Transform infrared spectroscopy (FTIR) measurements were performed with a NEXUS Thermo Nicolet FTIR spectrometer employing an attenuated total reflectance (ATR) accessory mod, Smart Performer. All spectra were obtained with a Ge crystal cell (maximum depth 0.8 μm). Spectra were normalized to the 1410 cm^{-1} peak before any data processing. Each spectrum reported is the average of at least three spectra measured in different areas of the film.

2.13. Modeling and Docking. The enzymes were modeled using the program YASARA Structure[36,37] applying the standard protocol. For the comparative modeling, the structure of *Streptomyces exfoliatus* lipase (PDB Code: 1JFR) with a sequence identity of 60% was used as a template.

The docking was performed using the program AutoDock 4.2[38] employing a genetic algorithm (20 individual runs, population size 150, number of generations 1850) and standard parameters. A molecular model of methyl acetate was used for the initial docking into the modeled structure of Thc_Cut2. The protonation and tautomerisation states of His residues were chosen according to hydrogen bonding networks. Asp, Glu, Arg, and Lys residues were treated as charged. A model of the substrate was built and optimized within YASARA. The substrate was prepared to be flexible whereas the protein model was kept rigid. The substrate cannot reach the ideal intermediate position for the covalent bond as the force field parameters of the serine will prevent the substrate to get closer to the oxyanion hole. Assuming that the carboxylic oxigen in its anionic form will fit into the oxyanion hole due to the flexibility of the residues the substrate will then be moved to a position to get covalently bound to the Ser-131, which brings the whole substrate to its tetrahedral intermediate. The best docking mode was used to build the covalent tetrahedral intermediate compound, which moved after a fast rough molecular mechanics calculation step into the right position. The substrate was modeled in its anionic form (formal charge of −1) and a restraint was introduced to the C atom to become covalently bound to the Ser-131 oxigen. The His-209 residue was modeled to be protonated and the covalently bound Ser-131 residue was set to have a formal charge of 0. This initial complex was subjected to an additional molecular mechanics optimization in YASARA using the AMBER03 force field and the standard optimization protocol. The energy-minimized complex was used to build and extend the tetrahedral intermediate to the 3PET substrate, and was also subjected to a molecular mechanics optimization following the protocol mentioned above.

Finally the complex of 3PET was extended by additional subunits of the polymer keeping the extensions as close as possible to the surface of the protein by keeping reasonable bond angles and dihedrals. This modeled substrate was again optimized but keeping the protein part fixed to exclude the influence to the protein by nearby placed substrate atoms. Thereafter, the minimization step was repeated with the whole complex. Surface hydrophobicity and

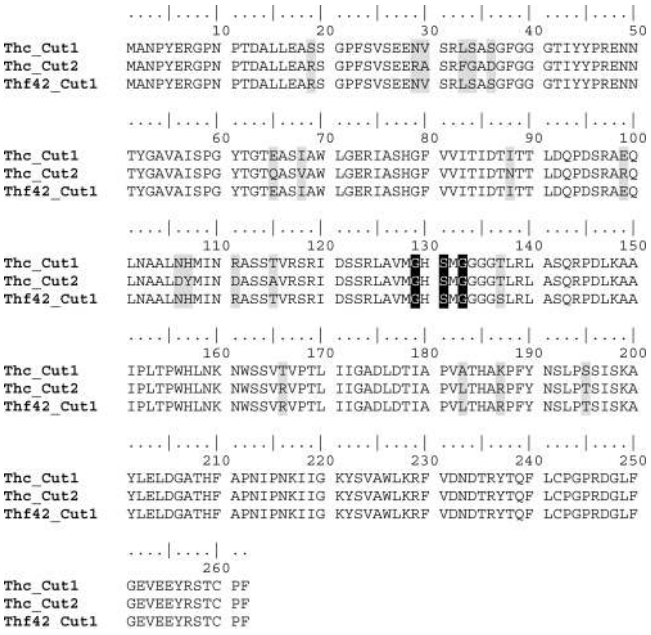

Figure 1. Alignment of amino acid sequences of cutinases isolated from *Thermobifida* strains without signal peptide. The conserved motif of the active site of serine hydrolases GxSxG is highlighted by a black background. Differences between sequences of the three cutinases are highlighted by a gray background.

electrostatic potential were generated using VASCo[39,40] and DelPhi.[41]

3. RESULTS

In many previous studies on PET hydrolysis, cutinases from two distinct *T. fusca* strains have been used. In a screening for more efficient PET-hydrolyzing *Thermobifida* cutinases the fact that we found out that very similar (i.e., homologous) enzymes showed different activities on PET intrigued us. Consequently, we cloned and expressed three highly homologous *Thermobifida* cutinases to study the effect of structural differences on hydrolysis of PET and of small molecules. Furthermore, we compared the activities of these enzymes to other PET-hydrolases.

3.1. Cloning, Heterologous Expression, and Sequence Analysis of Cutinases from *Thermobifida* Strains. On the basis of the genome sequences of cutinases from *T. fusca* strain YX, primers were designed for amplification of the homologous genes without signal peptide (amino acids 1−39 as determined by SignalP 3.0 software) by PCR from genomic DNA of *T. cellulosilytica* and *T. fusca*. A 6xHis encoding sequence was included in the reverse primer for expression of the enzymes as C-terminal His_6 fusion proteins. The obtained PCR-products (816 bp including 30 bp for the His_6 coding region) were cloned over the *Nde*I/*Hind*III restriction sites into vector pET26b(+) containing the T7 lac promoter for tight regulation of expression.

Analysis and comparison of the primary sequences (Figure 1) revealed that the cutinases were highly similar (94−99% homology) among each other differing in only 6 to 18 amino acids (Table 1). From *T. cellulosilytica* two cutinases were isolated, namely Thc_Cut1 and Thc_Cut2, which differ in 18 amino acids. From *T. fusca* one gene was isolated coding for Thf42_Cut1. Highest similarity was observed between Thc_Cut1 and Thf42_Cut1 (6 amino acid differences), the lowest between Thc_Cut1 and Thc_Cut2 (18 amino acid differences).

Table 1. Comparison of Cutinases from Two *Thermobifida* Species Based on Number of Different Amino Acids in the Primary Sequences

	Thc_ Cut1	Thc_ Cut2	Thf42_ Cut1	ThfKW3_ Cut1	ThfKW3_ Cut2
Thc_Cut1	0	18	6	15	2
Thc_Cut2		0	14	7	18
Thf42_Cut1			0	9	4
ThfKW3_Cut1				0	13
ThfKW3_Cut2					0

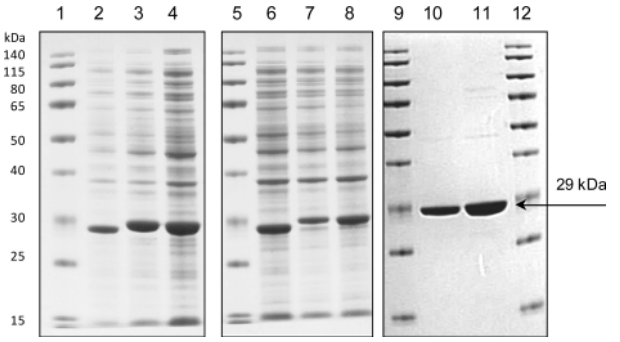

Figure 2. SDS−PAGE analysis (12%) of cutinases expressed in *E. coli* BL21-Gold(DE3) and purified by affinity−Tag. Samples were withdrawn after 20 h of induction at 20 °C, centrifuged, disrupted, and centrifuged again. Key: lanes 1, 5, 9, and 12, prestained protein molecular weight marker SM0671 (Fermentas); lanes 2, 3, and 4, soluble cell fraction of Thf42_Cut1, Thc_Cut1, and Thc_Cut2; lanes 6, 7, and 8, insoluble cell fraction of Thf42_Cut1, Thc_Cut1, and Thc_Cut2; lanes 10 and 11, purified Thc_Cut1 and Thc_Cut2.

Although the isolated genes feature a high GC content of about 68%, the cutinases were well heterologously expressed in *E. coli* BL21-Gold(DE3) without codon usage optimization for the host strain. Induction at 20 °C resulted in strong protein bands below 30 kDa as determined by SDS−PAGE analysis of the soluble and insoluble cell fractions which corresponded well to the calculated mass of 29.6 kDa (Thf42_Cut1), 29.4 kDa (Thc_Cut1), and 29.7 kDa (Thc_Cut2) for the tagged cutinases (Figure 2).

The cutinases from *T. fusca* and *T. cellulosilytica* were expressed intracellularly in the soluble, active form (Figure 2, lanes 2−4) and as inclusion bodies (Figure 2, lane 6 − lane 8). The cutinases were purified by the His_6-Tag technology to high purity as shown for Thc_Cut1 and Thc_Cut2 (Figure 2, lane 10 and lane 11). Typically, 10−15 mg purified enzyme was obtained from 100 mL cell culture. Interestingly, the *T. cellulolytica* cutinases Thc_Cut1 and Thc_Cut2 were identical in terms of aminoacid sequence to the cutinases Tfu_0883 and Tfu_0882 from *T. fusca* YX.[35]

3.2. Kinetic Characterization of the Cutinases on Soluble Substrates. In a first step, the kinetic parameters of the cutinases Thf42_Cut1, Thc_Cut1, and Thc_Cut2 on standard substrates PNPB and PNPA were determined. The K_m values of the three enzymes on PNPA and PNPB were in a similar range between 127 and 200 μmol L^{-1} and 1483 and 2133 μmol L^{-1} while the k_{cat} values varied in a range of 2 orders of magnitude (Table 2). In

dx.doi.org/10.1021/ma200949p |*Macromolecules* 2011, 44, 4632–4640

Table 2. Kinetic Parameters of the Thc_Cut1, Thf42_Cut1, and Thc_Cut2 Cutinases on Soluble Substrates

	PNPA		PNPB	
	K_m [μmol L^{-1}]	k_{cat} [s^{-1}]	K_m [μmol L^{-1}]	k_{cat} [s^{-1}]
Thc_Cut1	127 ± 12	211.9 ± 3.1	1483 ± 126	195.1 ± 26.9
Thf42_Cut1	167 ± 29	39.5 ± 3.0	2100 ± 361	30.9 ± 8.6
Thc_Cut2	200 ± 12	2.4 ± 0.2	2133 ± 416	5.3 ± 1.2

contrast to the cutinases, the PHA-depolymerase ePhaZmcl was active on longer chain model substrate like PNP palmitate but did not show any significant activity on PNPB and PNPA, (data not shown).

3.3. Hydrolysis of the Model Substrate 3PET. In order to obtain more mechanistic information regarding the mode of hydrolysis of the cutinases, the enzymes were incubated with the short chain model substrate 3PET. The water-soluble hydrolysis products BA, TA, MHET, HEB, BHET were quantified via HPLC (Figure 3). All *Thermobifida* enzymes cleaved endowise internal bonds of 3PET, which is reflected by the fact that high amounts of HEB but no BHET were found after 2 h of hydrolysis. Nevertheless, the enzyme concomitantly liberated exowise BA while after prolonged hydrolysis TA is liberated (only low amounts after 2 h). In case of Thc_Cut1, the stepwise hydrolysis of 3PET had proceeded further than for the other two enzymes leading to higher amounts of monomers (BA, TA) and of overall hydrolysis products. The PHA−depolymerase (ePhaZmcl) and ThfKW3_Cut1 released below 2 mmol of TA per mol or enzymes in total of mono- oligomers from 3PET while the amounts found for ThfKW3_Cut2 were comparable to those measured for Thf42_Cut1.

3.4. Hydrolysis of the PET Films. When incubated with PET films, the three cutinases released varying amounts of TA and MHET but no BHET (Figure 4). TA was the major hydrolysis product for Thc_Cut1 and Thf42_Cut1 whereas for Thc_Cut2, MHET was the most abundant product which may be hydrolyzed faster by the other two enzymes. In comparison, ThfKW3_Cut2 released 35.4 μmol of TA and 3.9 μmol of MHET per mole of enzymes while both the PHA−depolymerase (ePhaZmcl) and ThfKW3_Cut1 did not produce significant amounts hydrolysis products (data not shown).

The Water contact angle WCA after washing with surfactants was used to quantify hydrophilicity increases upon enzymatic surface hydrolysis of PET. Compared to the blank (74.2° ± 1.6°), the highest decrease of the WCA was observed for Thc_Cut1 (66.3° ± 2.7°) followed by Thf42_Cut1 (71.2° ± 0.9°). Thc_Cut2 did not decrease the hydrophobicity of PET films to a significant extent. Interestingly, the hydrophilicity increase obtained with the various cutinases correlated to the amount of hydrolysis products released from both PET and 3PET. An increased hydrophilicity as measured with WCA improves PET processing such as dyeing or coating with PVC.[42] For example, with the same cutinase (Thc_Cut1) and improved dyeing efficiency has been demonstrated for C.I. Basic Blue 3.[7]

Since the change of the WCA measured after treatment of PET with the Thf42_Cut1 was significant but rather low, further methods to estimate the degree of surface hydrolysis were employed. FTIR-ATR analysis revealed a significantly higher crystallinity index A_{1340}/A_{1410} of 0.290 when compared to the blank (0.260). In addition, the amount of carboxylic and hydroxylic

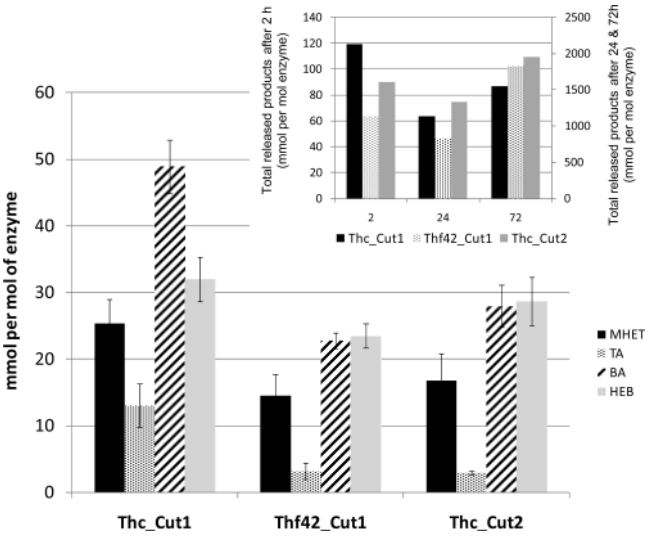

Figure 3. Hydrolysis (2 h of incubation) of 3PET with the cutinases Thf42_Cut1, Thc_Cut1, and Thc_Cut2 and total amount of hydrolysis products after different time intervals.

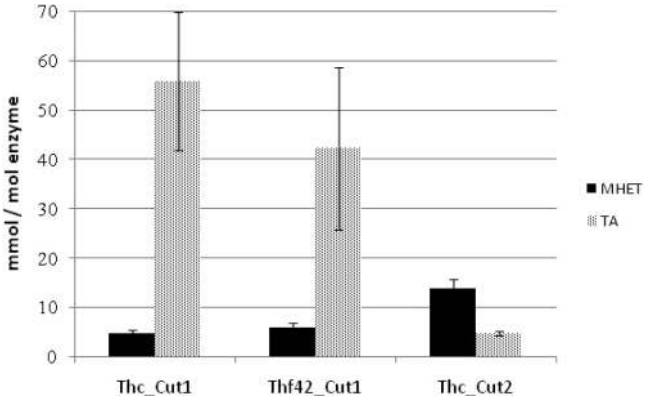

Figure 4. Hydrolysis of PET films using the cutinases Thc_Cut1, Thf42_Cut1, and Thc_Cut2.

groups generated at the PET surface were quantified via derivatization with 2-(bromomethyl)naphthalene (BrNP).[43]

Again, a significant increase of the fluorescence emission intensity from 950 to 1540 au after the esterfication was measured after treatment of PET with Thf42_Cut1.

3.5. Structure Function Comparison of Thc_Cut2 and Thc_Cut1. Out of the cutinases tested in this study, the *T. cellulosilytica* cutinases Thc_Cut2 and Thc_Cut1 showed the most pronounced activity differences on both soluble and insoluble substrates despite their remarkably high homology (93%). To correlate this behavior to structural differences models were created for both cutinases. As template structure chain A from *S. exfoliatus* lipase (PDB Code: 1JFR)[44] with a sequence identity of about 60% to the investigated proteins was used. As expected from sequence alignments, overall investigations of the models revealed that there are no significant differences close or at the proposed active site. However, the electrostatic potential and hydrophobicity on the surface differs in some regions in the vicinity of the active site.

In order to find whether the identified regions are able to influence the polymer binding behavior, we performed a docking

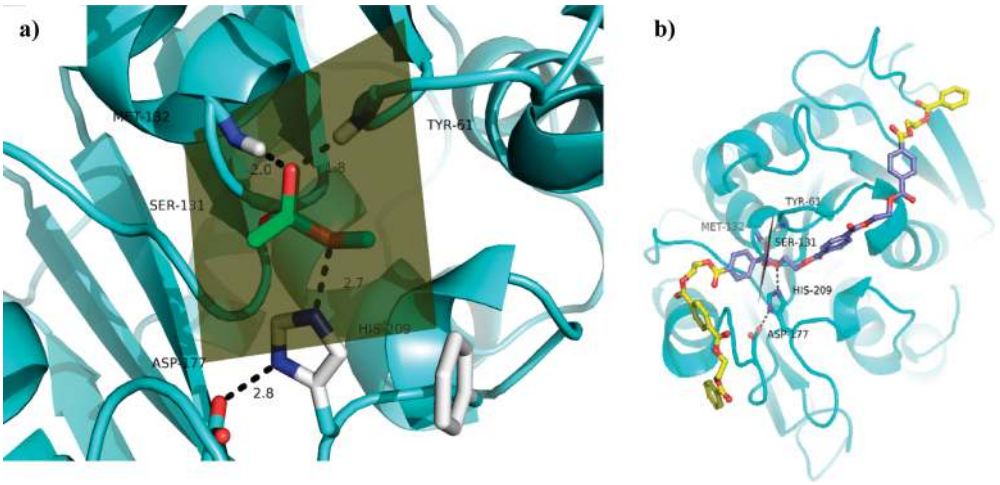

Figure 5. Modeled complex structures. (a) Active site view of the tetrahedral intermediate state of methyl acetate (green). A transparent plane is shown to illustrate the tetrahedral geometries. Active site residues are shown in stick representation. (b) Intermediate complex structure of the polysubstrate is shown. Active site residues are highlighted. The 3PET substrate part is colored in blue whereas the extensions with additional polymer subunits are in yellow. Figures were generated with PyMOL.

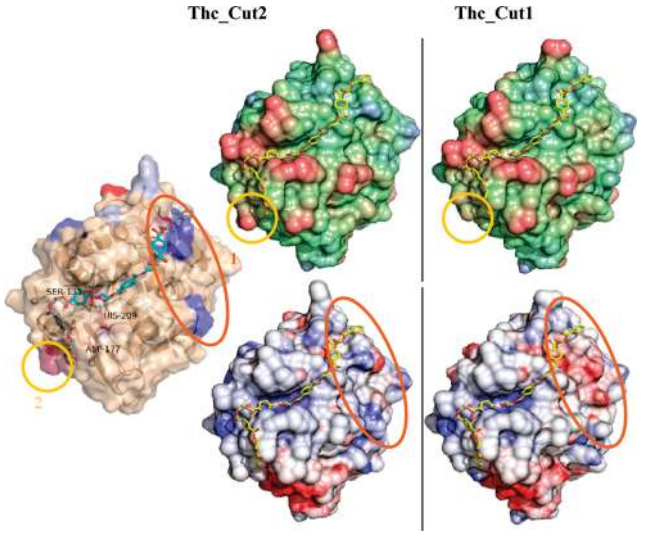

Figure 6. Surface comparison of two isomers. The modeled poly substrate is shown in yellow. The isomers Thc_Cut2 and Thc_Cut1 are separated with a black line. Representations of Thc_Cut2 are located at left and representations for Thc_Cut1 are on the right side of the black line. The hydrophobicity at the surface is shown on the top (from blue hydrophilic to green to red- hydrophobic) and the electrostatic potential (from red negative to blue positive) is shown below. Additional to the surface property comparisons, differences on surface residues are shown in the representation on the outer left. A gray surface indicates a different surface amino acid compared to Thc_Cut1 but with similar properties. Blue indicates residues which are not negatively charged compared to Thc_Cut1. A brown color indicates a more exposed hydrophobic amino acid compared to Thc_Cut1. The special regions 1 and 2 are indicated with colored circles. Figures were generated using PyMOL (The PyMOL Molecular Graphics System, Version 1.2r1, Schrödinger, LLC) and the VASCo Plug-In.

and a modeling step to mimic the covalently bound tetrahedral intermediate complex structure consisting of Thc_Cut2 and the poly substrate. (Figure 5, for details see material section). By spanning a plane across the Ser-131 O and the O- and C of the tetrahedral substrate intermediate, one can see that the active site His-209 which is supposed to be the hydrogen donor for the alcoholic product, is in the proximity of the O of the substrate (Figure 5a). This leads to the conclusion that the proposed complex which is shown in Figure 5 is in a position to form the degradation products. The oxyanion hole is formed by the helix where the active site Ser-131 is located and by the main chain NH of Met-132 and Tyr-61 which then stabilizes the anionic substrate complex.

Figure 6 shows differences in amino acids exposed to the surface between Thc_Cut2 and Thc_Cut1. Non essential differences are highlighted in gray whereas differences in surface residues, which contribute the most to the change of surface properties due to their complementary characters are highlighted in blue, red and brown. The comparison of surface properties in context with the modeled polymer revealed that it is possible that the polymeric substrate is able to reach the regions which differ in electrostatic and in hydrophobic surface properties (Figure 6). Two regions which had the most differences in surface properties could be identified (orange highlighted region 1 and yellow highlighted region 2 in Figure 6). Region 1 of Thc_Cut1 includes Ser19, Asn29, Val30, and Glu65, which are changed in Thc_Cut2 to the positively charged Arg19 and Arg29, the less hydrophobic Ala30, and uncharged Gln65. Region2 of Thc_Cut1 comprises Ala183 and Lys187 which are changed to a more hydrophobic Leu183 and Arg187 with a strong basic character in Thc_Cut2. All other amino acid alterations are far away from the modeled substrate intermediate or are at the N and C terminal regions of the sequence, all located at the opposite side of the protein (not shown).

4. DISCUSSION

PET-hydrolysis has been described for a small group of enzymes including bacterial cutinases from *T. fusca*[7] and *P. mendocina*[22] and fungal cutinases and lipases from *H. insolens*,[22,45] *F. solani*,[21,46] and *Thermomyces lanuginosus*[9] respectively. Interestingly, PET-hydrolysis activity even from highly similar (i.e., homologous) enzymes even from one and the same species greatly differs. To identify possible structural determinants for PET hydrolysis ability, three

closely related cutinases from two *Thermobifida* species were compared in this study.

The cutinases from *T. cellulosilytica* and from *T. fusca* were successfully cloned and expressed in *E. coli*. Despite the high homology of Thf42_Cut1, Thc_Cut1, and Thc_Cut2, these enzymes showed different *k*cat values for PNPB and PNPA differing in 2 orders of magnitude. Thc_Cut1 had the highest *k*cat values among the tested enzymes both on PNPB and PNPA, whereas the values for Thc_Cut2 were 100 times lower. The *k*cat values for Thf42_Cut1 were 10 times lower than Thc_Cut1. The measured *k*cat value of Thc_Cut1 on PNPB is in accordance with the one reported for the homologous cutinase Tfu_0883.[35] The *k*cat value of Thc_Cut2 was lower than that measured previously for the cutinase Tfu_0882 taking into account different assay conditions in terms of temperature.[35] On the other hand, the *k*cat value for a pNP esterase PNBCE from *Bacillus subtilis* was 720 s^{-1}.[47]

Upon incubation with the model substrate bis(benzoyloxyethyl) terephthalate (3PET) Thc_Cut1 released significantly higher amounts of soluble products MHET, TA, BA, and HEB than Tf42_Cut1 and Thc_Cut2 which released comparable amounts. This difference correlates with the kinetic parameters, being Thc_Cut1 the enzyme with the highest k_{cat} value. The pattern of oligomers and monomers released confirmed that all three enzymes were able to cleave internal ester bonds endowise and finally to completely hydrolyze 3PET. This is in contrast to a *T. lanuginosus* lipase where hydrolysis stopped at the stage of MHET.[9]

On PET films, out of all tested enzymes, only Thf42_Cut1 and Thc_Cut1 showed high hydrolysis activity at the identical enzyme dosage. In agreement with these results we and others have previously demonstrated that the cutinase from *T. fusca*, rTfH, hydrolyzed PET[9,48] which was found to be identical to Thc_Cut1 from *T. cellulosilytica* studied here. However, rTfH was produced in *E. coli* as fusion protein using the OmpA leader sequence and a His6 tag.[48] N-terminal sequencing revealed that cleavage of OmpA was not uniform and only small amounts of the recombinant hydrolase was cleaved at the expected site. Thus, previous results with these enzymes may not be directly comparable. Anyways, compared to PET-films used in this study, rTfH/Thc_Cut1 seem to be more active on PET-fibres.[9] Other authors[35] recently found that Tfu_0883 from *T. fusca*, which is identical to Thc_Cut1, was able to hydrolyze cyclic PET oligomers in contrast to another *T. fusca* cutinase termed Tfu_0882 (homologous to Thc_Cut2). Thus, these data are in agreement with higher activity on PET found for Thc_Cut1 in this study. Similarly, for the *T. fusca* strain KW3 we found considerably higher PET-hydrolysis activity for ThfKW3_Cut2 when compared to ThfKW3_Cut1 while the PHA-depolymerase ePhaZmcl showed only marginal amounts of hydrolysis products from PET. Apart from *Thermobifida* cutinases, a Thf_KW3 carboxylesterase had previously been reported to release 36.7 mol of TA per mol of enzyme from PET nanospheres after 24 h of incubation[26] but was not active on other PET substrates. TA was by far the dominant hydrolysis product from PET for all cutinases tested here. In previous studies on PET degradation with a cutinase from *H. insolens*, TA was likewise the major degradation product while no BHET and MHET were found.[22] On the other hand, Vertommen et al.[21] found predominantly MHET after treatment of PET with a cutinase from *F. solani* while Eberl et al.[9,20] found varying ratios of TA and MHPT/MHET released from PTT and PET depending on incubation time and material (fabrics, films) used.

Hydrophilicity increases can be attributed to endotype enzymatic PET surface hydrolysis as we have previously demonstrated with MALDI-TOF and XPS analysis[9] provided that all enzyme protein had been removed from the surface.[7,21] Consequently, the amount of small water-soluble molecules is not a prerequisite to yield hydrophilicity increases as previously demonstrated in a comparison of a cutinase and a lipase.[7,21] Nevertheless, in this study a correlation between released products from PET films and 3PET and hydrophilicity measured as decrease in the WCA was clearly demonstrated. Enzymes releasing more soluble products were able to increase the hydrophilicty of PET films to a higher extent. The degree of hydrophilisation achieved was not extraordinary but in the range of values reported previously for PET of the same crystallinity and a cutinase from *F. solani pisi*.[49]

Enzymatic treatment of PET with the novel Thf42_Cut1 lead to an increase of the crystallinity as documented by an increase of the A_{1341}/A_{1410} ratio measured via FTIR-ATR spectroscopy. Previously, with this technique a crystallinity increase was demonstrated for PET after treatment with a *F. solani pisi* cutinase.[49] The band at 1341 cm^{-1} is related with CH_2 wagging and is commonly used as indication of crystalline PET domains, whereas the band at 1410 cm^{-1}, is characteristic of the ring CC stretching[50−53] and is taken as reference band.[43] Therefore, the ratio between the intensity of both bands is commonly taked as indicator of the surface crystallinty. Generally, polyesterases have been reported to preferentially hydrolyze amorphous regions of PET.[7,9,21,49,54]

Recently, 10-fold activity of cutinases from *H. insolens*, *P. mendocina*, and *F. solani* on low-crystallinity PET (7% crystallinity) was demonstrated when compared with higher crystallinity (35%) PET.

Partial enzymatic surface hydrolysis should increase the amount of surfacial hydroxyl and carboxyl groups. Consequently, after alkylation with 2-(bromomethyl)naphthalene an increase of the fluorescence at 440 nm would indicate an increase of reactive hydroxyl or carboxyl groups.[49]

A significant increase from 950 to 1540 au in the fluorescene was measured for Thf42_Cut1. Similarly, derivatization of formed hydroxyl groups by sulphobenzoic acid anhydride has previously been used in monitoring enzymatic hydrolysis of PET.[42] On the other hand, XPS analysis has been used to demonstrate an increase in carboxyl and hydroxyl groups after enzymatic surface hydrolysis of PET.[9,20] One out of the three *Thermobifida* cutinases compared here, namely Thc_Cut1 was considerable more active on PET films and 3PET than the others. Thus, it was interesting to compare this enzyme with the least effective cutinase Thc_Cut2 in more detail. Substrate docking and modeling of the tetrahedral substrate-enzyme intermediate confirmed that the active site His-209 as hydrogen donor is indeed in the proximity of the O of the substrate allowing hydrolysis. Sequence alignment and modeling of Thc_Cut1 and Thc_Cut2 did not indicate significant differences close or at the proposed active site which could explain their different behavior in terms of PET hydrolysis. In contrast, previously, a comparison of the substrate specificities and structures of the *F. solani* and *A. oryzae* cutinases has revealed a preference of the latter enzyme to hydrolyze the polyester poly ε-(caprolactone) and longer chain substrates in general.[45] This difference has been explained with a deep continuous groove extending across the active site of the *A. oryzae* cutinase in contrast to that of *F. solani* with a shallow and interrupted groove. On the other hand, the active site of the *F. solani* cutinase had been engineered to better accept larger substrates which indeed resulted in higher activity on PET.[55]

For the two *T. cellulosilytica* cutinases investigated here, it seems that differences in electrostatic and hydrophobic surface properties in the vicinity to the active site could be responsible for different interactions with the modeled substrate intermediate. When compared to Thc_Cut1, one more positive charged region

and a second more hydrophobic region were identified for Thc_Cut2.

In conclusion we have cloned and characterized a new cutinase from *T. fusca* Thf42_Cut1 and cutinases from *T. cellulolysitica* (Thc_Cut1 and Thc_Cut2) and compared in terms of kinetic properties on model substrates and hydrolysis of PET. A correlation was found between kinetic parameters on soluble substrate, release of hydrolysis products from both 3PET and PET and the degree of PET hydrophylization. On the other hand, the highly homologous cutinases Thc_Cut1 and Thc_Cut2 showed distinct hydrolytic properties. Modeling of these enzymes revealed that differences in electrostatic and hydrophobic surface properties in the vicinity to the active site could be responsible for these differences.

AUTHOR INFORMATION

Corresponding Author

*E-mail: doris.ribitsch@acib.at. Telephone: +43 (316) 873 9341. Fax: +43 (316) 873 9343.

ACKNOWLEDGMENT

This study was performed within the Austrian Centre of Industrial Biotechnology ACIB, the MacroFun project and COST Action 868. This work has been supported by the Federal Ministry of Economy, Family and Youth (BMWFJ), the Federal Ministry of Traffic, Innovation and Technology (bmvit), the Styrian Business Promotion Agency SFG, the Standortagentur Tirol and ZIT - Technology Agency of the City of Vienna through the COMET-Funding Program managed by the Austrian Research Promotion Agency FFG. Financial support was also given from Sächsisches Staatsministerium für Umwelt und Landwirtschaft, Germany. PET was kindly provided by Dr. Vincent Nierstrasz from Ghent University.

REFERENCES

(1) Indest, T.; Strnad, S.; Kleinschek, K. S.; Ribitsch, V.; Fras, L. *Colloids Surf., A.* **2006**, *275* (1−3), 17–26.
(2) Karmakar, S. R. *Text. Sci. Technol.* **1999**, *12*, 1–48.
(3) De Geyter, N.; Morent, R.; Leys, C. *Nucl. Instrum. Methods Phys. Res., Sect. B* **2008**, *266* (12−13), 3086–3090.
(4) Vesel, A.; Mozetic, M.; Zalar, A. *Vacuum* **2007**, *82* (2), 248–251.
(5) Tressaud, A.; Durand, E.; Labrugère, C.; Kharitonov, A. P.; Kharitonova, L. N. *Fluorine Chem.* **2007**, *128* (4), 378–391.
(6) Zeronian, S. H.; Collins, M. *J. Text. Prog.* **1989**, *20* (2), 1–26.
(7) Brückner, T.; Eberl, A.; Heumann, S.; Rabe, M.; Gübitz, G. M. *J. Polym. Sci., Part A: Polym. Chem.* **2009**, *46* (19), 6435–6443.
(8) Kim, H. R.; Song, W. S. *Int. J. Cloth. Sci. Technol.* **2010**, *22* (1), 25–34.
(9) Eberl, A.; Heumann, S.; Brueckner, T.; Araujo, R.; Cavaco-Paulo, A.; Kaufmann, F.; Kroutil, W.; Guebitz, G. M. *J. Biotechnol.* **2009**, *143* (3), 207–212.
(10) Alisch, M.; Feuerhack, A.; Müller, H.; Mensak, B.; Andreaus, J.; Zimmermann, W. *Biocatal. Biotransform.* **2004**, *22* (5−6), 347–351.
(11) Guebitz, G. M.; Cavaco-Paulo, A. *Trends Biotechnol.* **2008**, *26* (1), 32–38.
(12) Müller, R. J.; Kleeberg, I.; Deckwer, W. D. *J. Biotechnol.* **2001**, *86* (2), 87–95.
(13) Ronkvist, Å. M.; Lu, W.; Feder, D.; Gross, R. A. *Macromolecules* **2009**, *42* (16), 6086–6097.
(14) Gübitz, G. M.; Cavaco-Paulo, A. *Curr. Opin. Biotechnol.* **2003**, *14*, 577–582.
(15) Nagarajan, V. US Patent 20050261465, May 24, 2005.
(16) Kellis T., J. Jr.; Ayrookaran J., P.; Mee-young, Y. US Patent 20020007518, January 24, 2002.
(17) Maurer, K.-H.; Michels, A.; Pütz, A.; Eggert, T.; Jager, K.-E. US Patent 11/989,927, October 15, 2009.
(18) Svendsen, A.; Schroder Glad, S. O.; Fukuyama, S.; Matsui, T. US Patent 6960459, November 1, 2005.
(19) Yoon, M. Y.; Kellis, J.; Poulouse, A. J. *AATCC Rev.* **2002**, *2* (6), 33–36.
(20) Eberl, A.; Heumann, S.; Kotek, R.; Kaufmann, F.; Mitsche, S.; Cavaco-Paulo, A.; Gübitz, G. M. *J. Biotechnol.* **2008**, *135* (1), 45–51.
(21) Vertommen, M. A. M. E.; Nierstrasz, V. A.; Veer, M. v. d.; Warmoeskerken, M. M. C. G. *J. Biotechnol.* **2005**, *120* (4), 376–386.
(22) Ronkvist, Å. M.; Xie, W.; Lu, W.; Gross, R. A. *Macromolecules* **2009**, *42* (14), 5128–5138.
(23) Silva, C. M.; Carneiro, F.; O'Neill, A.; Fonseca, L. P.; Cabral, J. S. M.; Gübitz, G.; Cavaco-Paulo, A. *J. Polym. Sci., Part A: Polym. Chem.* **2005**, *43* (11), 2448–2450.
(24) Nimchua, T.; Punnapayak, H.; Zimmermann, W. *Biotechnol. J.* **2007**, *2* (3), 361–364.
(25) Liebminger, S.; Eberl, A.; Sousa, F.; Heumann, S.; Fischer-Colbrie, G.; Cavaco-Paul, A.; Gübitz, G. M. *Biocat. Biotrans.* **2007**, *25* (2−4), 171–177.
(26) Oeser, T.; Wei, R.; Baumgarten, T.; Billig, S.; Föllner, C.; Zimmermann, W. *J. Biotechnol.* **2010**, *146* (3), 100–104.
(27) Sinsereekul, N.; Wangkam, T.; Thamchaipenet, A.; Srikhirin, T.; Eurwilaichitr, L.; Champreda, V. *Appl. Microbiol. Biotechnol.* **2010**, *86* (6), 1775–1784.
(28) Ihssen, J.; Magnani, D.; Thöny-Meyer, L.; Ren, Q. *Biomacromolecules* **2009**, *10* (7), 1854–1864.
(29) Korpecka, J.; Heumann, S.; Billig, S.; Zimmermann, W.; Zinn, M.; Ihssen, J.; Cavaco-Paulo, A.; Guebitz, G. M. *Macromol. Sym.* **2010**, *296* (1), 342–346.
(30) Heumann, S.; Eberl, A.; Pobeheim, H.; Liebminger, S.; Fischer-Colbrie, G.; Almansa, E.; Cavaco-Paulo, A.; Gubitz, G. M. *J. Biochem. Biophys. Methods* **2006**, *69* (1−2), 89–99.
(31) Billig, S.; Agrawal, P. B.; Nierstrasz, V. A.; Warmoeskerken, M. M. C. G.; Zimmermann, W. *COST 868 Workshop, Bratislava, Slovak Republic, 17−18 April*; 2008; p 17.
(32) Sambrook, J.; Fritsch, E. F.; Maniatis, T. *Molecular cloning: a labatory manual*, 2nd ed.; Cold Spring Harbor Laboratory Press: New York, 1989.
(33) Chen, S.; Tong, X.; Woodard, R. W.; Du, G.; Wu, J.; Chen, J. *J. Biol. Chem.* **2008**, *283* (38), 25854–25862.
(34) Laemmli, U. K. *Nature* **1970**, *227* (5259), 680–685.
(35) Chen, S.; Su, L.; Billig, S.; Zimmermann, W.; Chen, J.; Wu, J. *J. Mol. Catal. B: Enzym.* **2010**, *63* (3−4), 121–127.
(36) Krieger, E.; Koraimann, G.; Vriend, G. *Proteins Struct. Funct. Bioinf.* **2002**, *47* (3), 393–402.
(37) Krieger, E.; Darden, T.; Nabuurs, S. B.; Finkelstein, A.; Vriend, G. *Proteins Struct. Funct. Bioinf.* **2004**, *57* (4), 678–683.
(38) Morris, G.; Goodsell, D.; Halliday, R.; Huey, R.; Hart, W.; Belew, R.; Olson, A. J. *Comput. Chem.* **1998**, *19* (14), 1639–1662.
(39) Sanner, M. F.; Olson, A. J.; Spehner, J. C. *Biopolymers* **1996**, *38* (3), 305–320.
(40) Steinkellner, G.; Rader, R.; Thallinger, G.; Kratky, C.; Gruber, K. *BMC Bioinformatics* **2009**, *10* (1), 32.
(41) Honig, B.; Nicholls, A. *Science* **1995**, *268*, 1144–1149.
(42) Almansa, E.; Heumann, S.; Eberl, A.; Fischer-Colbrie, G.; Martinkova, L.; Marek, J.; Cavaco-Paulo, A.; Guebitz, G. *M. Biocatal. Biotransform.* **2008**, *26* (5), 365–370.
(43) Donelli, I.; Taddei, P.; Smet, P. F.; Poelman, D.; Nierstrasz, V. A.; Freddi, G. *Biotechnol. Bioeng.* **2009**, *103* (5), 845–856.
(44) Wei, Y.; Swenson, L.; Castro, C.; Derewenda, U.; Minor, W.; Arai, H.; Aoki, J.; Inoue, K.; Servin-Gonzalez, L.; Derewenda, Z. S. *Structure* **1998**, *6* (4), 511–519.
(45) Liu, Y. B.; Wu, G. F.; Gu, L. H. *AATCC Rev.* **2008**, *8* (2), 44–48.
(46) Alisch-Mark, M.; Herrmann, A.; Zimmermann, W. *Biotechnol. Lett.* **2006**, *28*, 681–685.

(47) Giver, L.; Gershenson, A.; Freskgard, P. O.; Arnold, F. H. *Proc. Natl. Acad. Sci. U.S.A.* **1998**, *95* (22), 12809–12813.
(48) Müller, R. J.; Schrader, H.; Profe, J.; Dresler, K.; Deckwer, W. D. *Macromol. Rap. Comm.* **2005**, *26* (17), 1400–1405.
(49) Donelli, I.; Freddi, G.; Nierstrasz, V. A.; Taddei, P. *Polym. Degrad. Stab.* **2010**, *95* (9), 1542–1550.
(50) Cole, K. C.; Guevremont, J.; Ajji, A.; Dumoulin, M. M. *Abstr. Pap. Am. Chem. Soc.* **1994**, *208*, 233-MSE.
(51) Dunn, D. S.; Ouderkirk, A. J. *Macromolecules* **1990**, *23* (3), 770–774.
(52) Stokr, J.; Schneider, B.; Doskocilova, D.; Lovy, J.; Sedlacek, P. *Polymer* **1982**, *23* (5), 714–721.
(53) Walls, D. J. *Appl. Spectrosc.* **1991**, *45* (7), 1193–1198.
(54) Herzog, K.; Müller, R. J.; Deckwer, W. D. *Polym. Degrad. Stab.* **2006**, *91* (10), 2486–2498.
(55) Araujo, R.; Silva, C.; O'Neill, A.; Micaelo, N.; Guebitz, G.; Soares, C. M.; Casal, M.; Cavaco-Paulo, A. *J. Biotechnol.* **2007**, *128* (4), 849–857.